Ultrasonics Sonochemistry 71 (2021) 105357

Contents lists available at ScienceDirect

Ultrasonics Sonochemistry

journal homepage: www.elsevier.com/locate/ultson

Ultrasonic treatment on physicochemical properties of water-soluble protein from *Moringa oleifera* seed

Shi-Qi Tang, Qiu-Han Du, Zhen Fu *

Institute of Light Industry and Food Engineering, Guangxi University, 53004 Nanning, China

ARTICLE INFO

Keywords:
Moringa oleifera seed
Protein
Structure
Physicochemical properties

ABSTRACT

Effect of ultrasonic power on the structure and functional properties of water-soluble protein extracted from defatted *Moringa oleifera* seed were explored. The results showed that ultrasonic treatment could reduce β-sheet and β-turn content of water-soluble protein from *Moringa oleifera* seed (MOWP) and increase the content of random coil and α-helix. Changes in intrinsic fluorescence spectra, surface hydrophobicity (H_0) and thermal behaviors indicated that ultrasonic had significant effect on the tertiary structure of MOWP. The results of SEM and SDS-PAGE showed that the MOWP was aggregated but not significantly degraded by ultrasound. The solubility, foaming properties and emulsifying properties of MOWP increased firstly and then decreased with the increase of ultrasonic power. Ultrasonic treatment altered the functional properties of MOWP, which might be attributed to the exposure of hydrophilic group and the change of and secondary and tertiary structure.

1. Introduction

Moringa oleifera, also known as the "drumstick tree", is native to the tropical and southern subtropical regions of northern India [1]. *Moringa oleifera* seed (MOS), as a derivative product of *Moringa oleifera*, is extremely rich in nutrients, contains a large amount of fat, protein, mineral elements and dietary fiber, and is known as "plant diamond" [2–5]. The multiple uses of MOS have gradually been drawing more and more attentions. In Southeast Asian countries, MOS was used as a traditional folk medicine to prevent and treat a variety of diseases [6]. In the food industry, MOS could be used as an auxiliary material to increase the nutritional content of food [4,6]. MOS contains considerably good quantity of high-quality protein (~52%), which has all the essential amino acids [7]. *Moringa oleifera* seed protein may be a potential functional protein and can be used as an alternative to other proteins for human food use due to its balanced amino acid profile [7]. Hence, the structure, function and nutritional characteristics of the protein from MOS are of great significance for its related development [1,7–9].

In recent years, ultrasonic technology has been widely used in food processing, especially in protein modification, due to its environmentally friendly and low-cost advantages [10]. The works on ultrasonic modification of proteins have been widely investigated [10–22]. Generally, cavitation effects generated by ultrasound could alter molecular structure and spatial conformation of protein, resulting in the improvement of functional properties of protein such as solubility, emulsifying and foaming properties [10–14]. However, Currently, there are few reports on ultrasonic modification of MOWP.

The purpose of this study was to investigate the effect of ultrasonic power on the structure and functional properties of MOWP. MOWP were treated with different ultrasonic power and the changes in secondary structure and tertiary structure were analyzed by Fourier transform infrared spectroscopy (FTIR), fluorescence spectrophotometer and sodium dodecyl sulphate–polyacrylamide gel electrophoresis (SDS-PAGE), respectively. In addition, functional properties including solubility, emulsifying and foaming properties were evaluated.

2. Materials and methods

2.1. Raw materials

Commercial MOS (Guangxi, China) were smashed and passed through 80 mesh sieve. After that, the MOS flour was degreased by *n*-hexane; then dried and stored in a drier for the follow-up experiments.

2.2. Preparation of MOWP

According to the method of Kim et al. [23], the defatted MOS flour was dispersed in distilled water (1:25) and continuously stirred for 2.5 h

* Corresponding author.
E-mail address: fuzhen13@gxu.edu.cn (Z. Fu).

https://doi.org/10.1016/j.ultsonch.2020.105357
Received 6 August 2020; Received in revised form 15 September 2020; Accepted 24 September 2020
Available online 7 October 2020

at room temperature (S25, German IKA company, Guangzhou, China), and then centrifuged at 8000 r/min at 4 ℃ for 25 min (CR21N, Himac, Tokyo, Japan). The supernatant was taken for reserve. The extraction process was repeated. The supernatant was precipitated by isoelectric precipitation (pH 4.5). After isoelectric point precipitation, the solution was centrifugated at 8000 r/min at 4 ℃ for 25 min. The sediment was dialyzed for 36 h. After dialysis, Protein of MOS (MOWP) was obtained by lyophilization (FD-1D-50, Beijing Boyikang Experimental Instrument Co., Ltd., Beijing, China). The purity of MOWP was 93.84 ± 1.32% by HPLC.

2.3. Ultrasonic treatment of MOWP

MOWP (1 g (db)) was added to 100 mL PBS buffer (20 mmol/L, pH 7.0) and stirred in a magnetic stirrer for 2 h at room temperature. Then the beaker was placed in an ice bath. Aqueous solution of the protein (1% w/v) was treated by an ultrasonic generator (TL-650Y, Jiangsu Tianling Instrument Co., Ltd., Yancheng, China). The power was set at different amplitudes (0%, 20%, 40%, 60%, 80% and 100%) and the corresponding values were 0, 130, 260, 390, 520, and 650 w, respectively. The probe was placed below the liquid level of 20 mm and the ultrasonic treatment time was 15 min (working for 3 s, stop for 2 s); and the sample beaker was placed in an ice-water mixture during ultrasonic treatment to avoid excessive rise in temperature. The ultrasonic treated MOWP samples were obtained by dialysis and lyophilization.

2.4. Fourier-transform infrared spectroscopy (FTIR) analysis

Potassium bromide was taken into a 105 ℃ oven to a balanced weight. The sample and potassium bromide (1: 100 (g/g)) were fully ground and mixed, and compressed in a vacuum. FTIR spectra (TENSOR II, BRUKER OPTICS, Germany) was collected in the range from 4000 to 400 cm^{-1} during 32 scans, with a resolution of 4 cm^{-1} at ambient condition. Further analysis of infrared absorption band (amide I band, 1600–1700 cm^{-1}) and secondary structure of protein was carried out by deconvolution and second derivative treatment in Omnic 8.2 software (ThermoFisher scientific, USA) and the secondary protein structure contents were calculated.

2.5. Scanning electron microscopy analysis

MOWP was simply deposited onto carbon tape stuck on a specimen holder and coated with a thin film of gold in a vacuum evaporator. The obtained specimens were observed in a scanning electron microscope (Phenom Pro 05, Phenom, Netherlands) at high voltage (10 kV) to determine the morphology of freeze-dried MOWP samples.

2.6. Sodium dodecyl sulphate–polyacrylamide gel electrophoresis (SDS-PAGE) analysis

SDS-PAGE was performed using an electrophoresis system (Bio-Rad Laboratories, Inc., Hercules, USA) with a 12% separating gel and a 5% stacking gel. The Marker loading volume was 5 μL/lane and the sample loading volume was 10 μL/lane. the voltages of the concentration gel and separation gel were 80 V and 120 V, respectively [23]. After electrophoresis, the gel was stained with Coomassie Brilliant Blue Ultrafast staining solution for 0.5 h and imprinted by a fluorescence imaging System (ChemiDoc MP System, BIO RAD, Shanghai, China)

2.7. Intrinsic fluorescence analysis

The intrinsic fluorescence was determined by a fluorescence spectrometer (RF-5301PC, Shimadzu Corporation, Tokyo, Japan). The MOWP solution (0.2 mg/mL) were dissolved in PBS buffer (50 mmol/L, pH7.0). The excitation wavelength was 290 nm and the emission wavelength range were 300 ~ 500 nm [24].

2.8. Surface hydrophobicity (H_0) measurement

H0 of MOWP was determined according to the method of Pham et al. [25] with some modification. The MOWP solution was prepared by dissolving the powder in PBS buffer (20 mmol/L, pH 7.0). Then the dispersions were centrifuged at 1000 × g for 10 min and their supernatants were collected. A serial dilution of the supernatant was carried out to obtain 0.005–0.5 mg/mL protein concentration. Subsequently, 50 μL of 8 mM 1-anilino-8-naphthalene-sulfonate (ANS) solution, prepared in the same buffer solution, was added to 2 mL of the sample solution and the mixture was incubated at ambient temperature for 45 min. The fluorescence intensity of the sample was measured, the excitation wavelength was 390 nm, the emission wavelength was 470 nm, and the slit was 5 nm. The regression curves of fluorescence intensity and sample solution mass concentration were drawn to obtain the linear regression slope, and the initial slope was H_0.

2.9. Thermal properties

The thermal properties of different samples were determined by differential thermal scanning (DSC) (DSC200PC, Netzsch Instruments, Germany). About 3 mg MOWP were weighed and placed in an aluminum sample pans for DSC scanning, and heated from 25 °C to 180 °C at a rate of 10 °C/min [24].

2.10. Protein solubility measurement

The solubility of MOWP was determined by the method of Ling with slight modification [24]. The MOWP sample (1 wt%) was dispersed in PBS buffer (20 mmol/L, pH 7.0). The supernatant was obtained by stirring for 2 h at room condition and centrifugation (8000 r/min at 4 ℃ for 15 min) Bradford's method [26] was used to measure the protein content in the supernatant. The MOWP solubility was expressed as grams of soluble protein per 100 g of MOWP.

2.11. Foaming properties

Foaming activity index (FAI) and stability index (FSI) were also measured at pH 7.0 according to the method of Arte et al. [27] with some modification. 30 mL MOWP solution (1 mg/mL) was placed in a 100 mL cylinder. The protein solution was homogenized for 2 min at a rotating speed of 10,000 r/min (AD500S-H, Suzhou Jiangdong Precision Instrument Co., Ltd., Pingjiang, China), recording the volume of the solution as V1. The volume of the solution was recorded again after 30 min as V2. The FAI and FSI were calculated as follows:

$$FAI(\%) = \frac{V1 - 30}{30} \times 100\% \quad (1)$$

$$FSI(\%) = \frac{V2}{V1} \times 100\% \quad (2)$$

2.12. Emulsifying properties

The emulsifying properties of MOWP were determined by referring to the method of Li et al. with some modifications [28]. The MOWP sample were diluted with PBS buffer (20 mmol/L, pH 7.0). Then 30 mL MOWP solution and 10 mL soybean oil were mixed and homogenized at a speed of 10,000 r/min for 2 min. After that, 50 μL emulsion was collected from the bottom of the solution immediately (0 min) or 10 min after homogenization and 5.0 mL SDS solution (0.1%) was added and shaken well. The absorbance was measured using a Visible light spectrophotometer (UV-2700, Shimadzu Corporation, Shanghai, China) at 500 nm. Emulsification activity index (EAI) and emulsification stability index (ESI) were calculated as follows:

$$\mathrm{EAI}(mg/mL) = \frac{2.303 \times 2 \times A0 \times N}{C \times (1-\varphi)} \quad (3)$$

$$\mathrm{ESI}(\mathrm{min}) = \frac{Ao}{A0 - A10} \times 10 \quad (4)$$

where N is the dilution factor of the emulsion ($N = 100$), C is the mass concentration of the sample ($C = 2$ mg/mL), φ is the volume fraction of the aqueous phase in solution ($\varphi = 0.75$), and A0 and A10 are the absorbance of the diluted emulsion at 0 and 10 min, respectively.

2.13. Statistical analysis

The experiments were repeated in triplicate. The data were expressed as mean ± standard deviation. The results were drawn using Origin 9.1 and analyzed by IBM SPSS Statistics 20 software.

3. Results and discussion

3.1. FTIR analysis

FTIR was used to characterize the secondary structure of MOWP and ultrasound-treated samples. The amide I band (1700 ~ 1600 cm^{-1}) was evaluated [24]. FTIR spectrum of MOWP treated or untreated by ultrasound was displayed in Fig. 1. There was a characteristic peak at 1658 cm^{-1} in amide I band, which belonged to α-helix and no change after ultrasonic treatment, indicating that there was no hydrogen bond fracture. As the ultrasonic power increased, the peak width in the amide I band was significantly increased, suggesting that the ultrasonic treatment power, especially at 40% and 60%, enhanced – C═O stretching vibration of MOWP. The MOWP conformation was effectively changed and resulted in a relatively stable structure under 40% and 60% ultrasonic powers.

The peaks in the amide I band corresponding to the secondary protein structures was as follows: β-sheet (1610 ~ 1640 cm^{-1})、β-turn (1640 ~ 1645 cm^{-1})、random coil (1650 ~ 1660 cm^{-1})、α-helix, (1661 ~ 1700 cm^{-1}). The secondary protein structure contents were shown in Table 1. The secondary structure of MOWP was mainly composed of β-sheets and β-turns.

Compared with the untreated MOWP, the contents of β-sheet and β-turn of the ultrasound-treated samples were firstly decreased and then increased. The α-helix and random coil content were increased and then reduced with the increasing ultrasonic power. This might be due to the fracture of some secondary bond of β-sheets and β-turns and rearranged into random coil and α-helix. The transformation was the highest by 40% ultrasonic power treatment. With further increasing the ultrasonic power, the peak value did not significantly change.

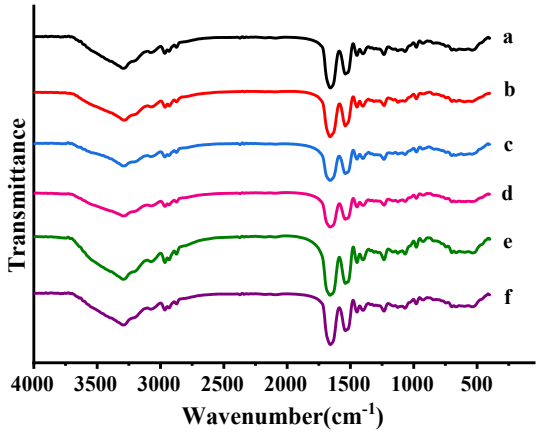

Fig. 1. FTIR spectrum of MOWP- treated by ultrasound: a, 0% ultrasonic power; b, 20% ultrasonic power; c, 40% ultrasonic power; d, 60% ultrasonic power; e, 80% ultrasonic power; f, 100% ultrasonic power.

Table 1
Effect of ultrasonic power on secondary structure of protein.

Ultrasonic power (%)	Protein secondary structure content (%) β-sheet	Random coil	α-helix	β-turn
0	44.78 ± 0.93^{c}	0.17 ± 0.11^{a}	1.82 ± 1.13^{a}	53.22 ± 0.39^{d}
20	42.82 ± 0.77^{b}	2.53 ± 0.22^{b}	9.22 ± 1.43^{d}	45.42 ± 0.66^{a}
40	38.57 ± 0.86^{a}	3.23 ± 0.57^{c}	7.72 ± 0.95 ^{cd}	50.48 ± 0.94^{c}
60	43.96 ± 0.71^{bc}	2.07 ± 0.31^{b}	5.77 ± 0.86^{bc}	48.19 ± 1.23^{b}
80	45.02 ± 0.92^{c}	2.15 ± 0.14^{b}	5.01 ± 1.23^{b}	47.82 ± 0.47^{b}
100	44.28 ± 1.04^{bc}	0.32 ± 0.17^{a}	2.33 ± 1.11^{a}	53.07 ± 0.34^{d}

There is a significant difference between the probability level of 5% lowercase letters and the difference between the different letters.

3.2. SEM analysis

As shown in Fig. 2A, microstructure of MOWP was obviously changed by ultrasonic treatment. The untreated MOWP was composed of irregularly small particles with loose structure. After ultrasonic treatment, the MOWP became more compact, but there seems to be no significant change in the shape and particle size of the MOWP. With the increase of ultrasonic power (Fig. 2B ~ F), the degree of protein molecular aggregation was increased, which might be due to the exposure of hydrophilic groups caused by ultrasound. The higher the ultrasonic power, the stronger the hydrophilic groups were aggregated into the network, ultimately affecting its functional properties. The results of the change in the microstructure of MOWP after ultrasonic treatment was similar with the published results of rice protein isolates treated by radio frequency treatment [24]. Dong et al. [12] also reported that high-power ultrasonic treatment could promote the aggregation of soybean protein isolates and increased the size of protein molecules. However, it is reported that low frequency and low-power ultrasound treatment could loosen the structure of various proteins such as corn glutelin, which resulted in exposure of the hydrophobic groups embedded in the molecule and increasing surface hydrophobicity of corn glutelin [24].

3.3. SDS-PAGE and intrinsic fluorescence

The distribution of molecular weight of MOWP treated by ultrasonic treatment were revealed by SDS-PAGE and shown in Fig. 3A. The results showed that ultrasonic treatment had no significant influences on the molecular weight of MOWP. In the range of 14.4 ~ 180.0 kDa, there were multiple subunit bands, indicating that MOWP contained disulfide bonds. The main subunit bands of MOWP at 13.0 kDa and 25.0 ~ 35.0 kDa. however, after ultrasonic treatment a few subunit bands of 48.0 kDa and 56.0 kDa appeared. This might due to be the aggregation of MOWP resulted from ultrasonic cavitation. The results showed that MOWP could not be degraded by ultrasound, and the protein molecules could be aggregated to form larger molecular weight proteins, which was consistent with the SEM results.

The conformation and tertiary structure of MOWP treated by ultrasound were further characterized by Intrinsic fluorescence and shown in Fig. 3B. The peak values (λ_{max}) of the samples treated with different ultrasonic power were shifted; and as ultrasonic power increased, the λ_{max} increased firstly and then decreases. The maximum λ_{max} of MOWP treated with 40% ultrasonic power reached 353 nm. The peak shift of the crest indicated that the tertiary structure of MOWP had been changed during the ultrasonic treatment. When the ultrasonic power was increased up to 100%, the MOWP tertiary structure was stretched

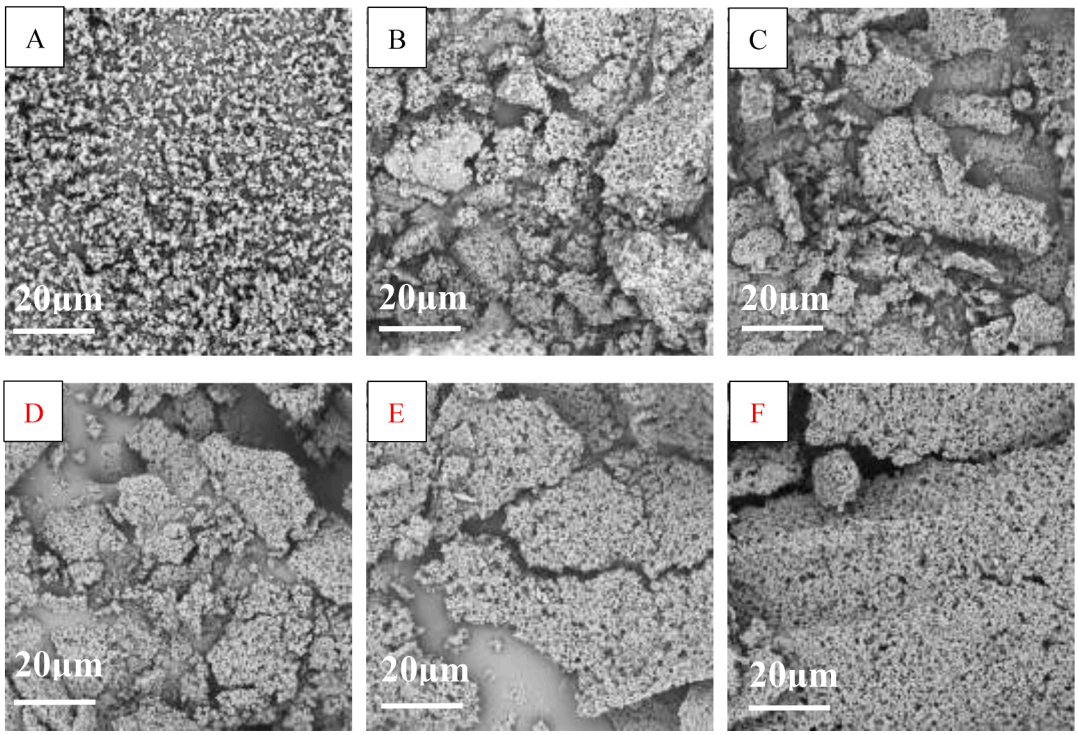

Fig. 2. Effects of ultrasonic power on surface microstructure of MOWP. A,0% ultrasonic power; B,20% ultrasonic power; C,40% ultrasonic power; D,60% ultrasonic power; E, 80% ultrasonic power; F,100% ultrasonic power.

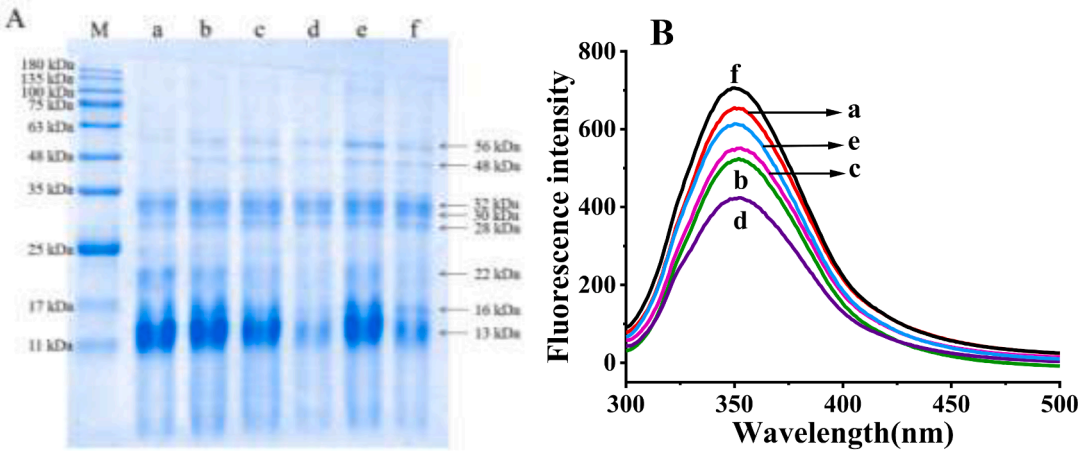

Fig. 3. SDS-PAGE pattern (A), intrinsic fluorescence spectra (B) of MOWP treated by ultrasound. M, Molecular weight standard; a, 0% ultrasonic power; b, 20% ultrasonic power; c, 40% ultrasonic power; d, 60% ultrasonic power; e, 80% ultrasonic power; f, 100% ultrasonic power.

and the fluorescence intensity was the strongest due to the more exposure of chromophoric groups. There were relatively large differences in the change of intrinsic fluorescence between MOWP and other proteins, such as chicken bone protein [12] and plum seed protein isolate [15], when processed by ultrasonic treatment. Probably the prime reason was that the secondary structure contents were different, which resulted in different effects of ultrasound treatment on different protein.

3.4. Surface hydrophobicity (H_0)

The H_0 of proteins was an indication that the number of exposed hydrophobic groups on the surface of protein molecules were available for bonding, which was important for protein stability and conformation and influence protein functionality [11,14]. The influences of ultrasonic power on the H_0 of MOWP were displayed in Fig. 4. The results showed that the H_0 of MOWP firstly decreased and then increased with increasing ultrasonic treatment power. Under the condition of 40% and 60% ultrasonic power, the H_0 values were lowest. Stathopulos et al. [29] reported that H_0 of bovine serum protein treated by ultrasound was enhanced due to the gradual exposure of hydrophobic group. Ren et al. [11] reported that H_0 of soy protein isolate treated by ultrasound was increased because large aggregates in soy protein isolate were dissociated, which increased the exposure of hydrophobic regions. H_0 values of whey protein [21] and wheat germ protein [13] treated by ultrasound were also increased. The difference in H_0 induced by ultrasound between MOWP and other proteins might due to the difference in structure. Meanwhile, cavitation effect led to a relatively high content of random coil and more the hydrophilic groups embedded in protein were

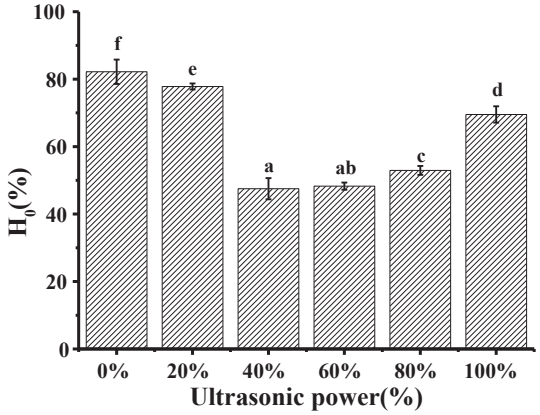

Fig. 4. Effects of ultrasonic power on H_0 of MOWP.

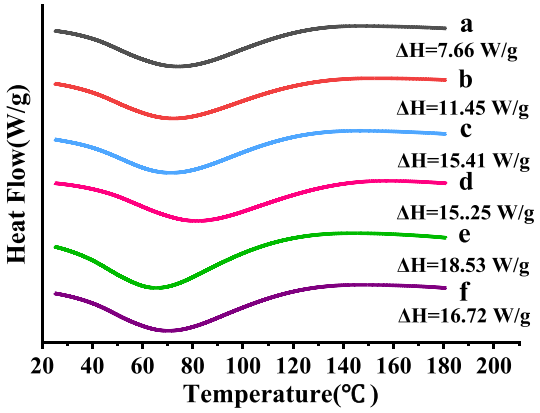

Fig. 5. Effects of ultrasonic power on thermal properties of MOWP. a, 0% ultrasonic power; b, 20% ultrasonic power; c, 40% ultrasonic power; d, 60% ultrasonic power; e, 80% ultrasonic power; f, 100% ultrasonic power.

gradually exposed. When the ultrasonic intensity reached its maximum, the molecular structure of the protein was rearranged, the hydrophobic groups were re-exposed, and the H_0 of MOWP was increased again. The changes of H_0 indicated that the tertiary structure of MOWP was altered significantly by ultrasonic treatment and suggested MOWP was different from other proteins in structure and functional characteristics.

3.5. Thermal properties

The DSC curves of MOWP were shown in Fig. 5. The thermal denaturation temperature (T_d) commonly indicates the thermal stability of a protein, while enthalpy (ΔH) represents the extent of ordered structure of a protein [24]. Compared with the untreated sample, the ΔH of MOWP treated by ultrasonic treatment was significantly ($p < 0.05$) increased, suggesting that ultrasonic treatment improved the ordered structure of MOWP. The reason might be that the cavitation effect induced MOWP to agglomerate and altered the tertiary structure of MOWP. This result showed that ultrasonic treatment could disrupt the hydrogen bond and hydrophobic interactions, and the extent of disruption was increased with increasing the power. As the further increase of ultrasonic power, the MOWP structure might be rearranged to a certain extent. The DSC result further confirmed that ultrasonic cavitation led to the spatial structure of MOWP, which could affect the functional properties of the protein [14].

Table 3
Effect of ultrasonic treatment of MOWP on functional properties.

Property	Ultrasonic power (%) 0	20	40	60	80	100
Protein solubility (%)	5.56 ± 0.66^{a}	9.14 ± 3.37^{a}	14.63 ± 1.33^{b}	30.53 ± 4.30^{d}	28.47 ± 3.70^{c}	24.07 ± 1.36^{c}
FAI(%)	12.39 ± 2.89^{a}	14.83 ± 1.13^{ab}	22.27 ± 3.05^{c}	16.74 ± 1.97^{ab}	17.67 ± 3.61^{b}	14.84 ± 1.15^{ab}
FSI(%)	93.94 ± 2.75^{b}	90.14 ± 1.13^{b}	84.36 ± 2.23^{a}	89.61 ± 2.56^{b}	87.99 ± 0.59^{b}	90.72 ± 1.05^{bc}
EAI(mg/mL)	60.90 ± 3.45^{b}	74.72 ± 3.23^{d}	79.63 ± 1.75^{e}	73.29 ± 1.55^{d}	68.27 ± 1.58^{c}	54.76 ± 2.04^{a}
ESI(min)	20.08 ± 1.77^{d}	14.29 ± 0.49^{b}	12.75 ± 0.30^{ab}	11.60 ± 0.59^{a}	13.43 ± 0.57^{b}	18.21 ± 0.50^{c}

There is a significant difference between the probability level of 5% lowercase letters and the difference between the different letters.

3.6. Solubility

The solubilities of MOWP treated by ultrasonic treatment were displayed in Table 3. The solubility of native MOWP is 5.56%. Ultrasonic treatment increased the solubility of MOWP significantly($P < 0.05$). As the ultrasonic power increased, the solubilities of treated MOWP were increased from 5.56% to 30.53%. When the ultrasonic power reached to 60%, the solubility was highest and the values was 30.53%. With further increase in ultrasonic power, the solubilities slightly decreased from 30.53% to 24.07%. This might be due to that the conformation was altered and the molecules structure of MOWP was stretched by ultrasonic treatment, which resulted in more hydrophilic groups exposure. Meanwhile, the increase in water solubility may also be owing to formation of soluble protein aggregates [18], which was confirmed by the results of SDS-PAGE and SEM. The change in λ_{max} in the intrinsic fluorescence spectroscopy analysis was also an indication that ultrasonic cavitation changed the MOWP tertiary structure, suggesting that ultrasound treatment could disrupt some of the non-covalent interactions of protein, such as hydrogen bonds and hydrophobic interactions, which could improve protein solubilities [11]. These results were similar with the published results of soybean protein isolate [30] and pea protein[18] that the ultrasonic effect could improve the solubility of protein. In addition, the increase in solubility would result in the improvement of emulsifying property and foam capacity.

3.7. Foaming properties

Protein foaming is an important functional property to evaluate in food processing. Protein foaming performance mainly depends on protein surface activity and film forming. The FAI and FSI of MOWP was also displayed in Table 3. the FA of MOWP was significantly ($p < 0.05$) improved and then reduced with increasing of the ultrasonic power. The of FAI of treated MOWP (40% power) was highest and the FAI value was 22.27%. however, the change trend of FSI of MOWP was opposite to the FAI trend. The values of FSI were decreased from 93.94% to 84.36% and then increased from 84.36% to 90.72%. The reason was that ultrasonic cavitation increased the solubility of MOWP, and the foaming capacity was enhanced when the soluble protein increased, but the stability of foaming was reduced when the surface activity decreased. Jambrak et al. [31] also reported that ultrasonic treatment improved the FAI of whey protein and reduced its FSI.

3.8. Emulsifying properties

As shown in Table 3, EAI of MOWP was significantly increased from

60.90 mg/mL to 79.63 mg/mL ($p < 0.05$) with the increase of ultrasonic power. With further increased the power, the EAI of MOWP was significantly reduced to 54.76 mL/mL ($p < 0.05$). The ESI of MOWP was significantly decreased by ultrasonic treatment ($p < 0.05$). It is reported that an increase in the solubility and H_0 of protein resulted in higher emulsifying properties [32,33]. The above results showed that the changing trend of EAI was consistent with the trend of solubility and H_0. Moreover, the FTIR results showed that the β-sheets and β-turns in MOWP were converted into random coil. Therefore, Ultrasonic treatment altered the emulsifying properties of MOWP, which might be attributed to the change of aggregates, solubility, H_0, and secondary structure [11]. Chen et al [34] reported similar conclusions that ultrasonic power improved protein emulsification. Similar results were also reported [32,35–36]. Yang et al. [37] also confirmed that the change of H_0, secondary structure and solubility would result in the improvement of emulsifying properties for protein.

4. 4.Conclusions

MOWP was mainly composed of β-sheets and β-turns. Ultrasonic treatment could induce the changes of secondary and tertiary structure of MOWP. Ultrasonic treatment could reduce β-sheet and β-turn content of MOWP and increase the content of random coil and α-helix. The MOWP was aggregated but not significantly degraded by ultrasound. The solubility, foaming properties and emulsifying properties of MOWP increased firstly and then decreased with the increase of ultrasonic power. The exposure of hydrophilic group and the change of and secondary and tertiary structure were responsible for functional properties of MOWP treated by ultrasound. Ultrasonic treatment could effectively improve the thermal stability of MOWP. These results would provide a useful theoretical basis for understanding the mechanism of ultrasonic treatment on MOWP and its potential application in food processing.

Declaration of Competing Interest

The authors declare that they have no known competing financial interests or personal relationships that could have appeared to influence the work reported in this paper.

Appendix A. Supplementary data

Supplementary data to this article can be found online at https://doi.org/10.1016/j.ultsonch.2020.105357.

References

[1] T.A. Aderinola, A.M. Alashi, I.D. Nwachukwu, T.N. Fagbemi, V.N. Enujiugha, R. E. Aluko, In vitro digestibility, structural and functional properties of Moringa oleifera seed proteins, Food Hydrocolloids 101 (2020) 105574, https://doi.org/10.1016/j.foodhyd.2019.105574.

[2] R.W. Saa, E.N. Fombang, E.B. Ndjantou, N.Y. Njintang, Treatments and uses of Moringa oleifera seeds in human nutrition: A review, Food Science & Nutrition 7 (2019) 1911–1919.

[3] P.H.F. Cardines, A.T.A. Baptista, R.G. Gomes, R. Bergamasco, A.M.S. Vieira, Moringa oleifera seed extracts as promising natural thickening agents for food industry: Study of the thickening action in yogurt production, Lwt 97 (2018) 39–44.

[4] F. Anwar, S. Latif, M. Ashraf, A.H. Gilani, Moringa oleifera : a food plant with multiple medicinal uses, Phytotherapy Research Ptr 21 (2007) 17–25.

[5] A. Leone, A. Spada, A. Battezzati, A. Schiraldi, J. Aristil, S. Bertoli, Moringa oleifera Seeds and Oil: Characteristics and Uses for Human Health, Int. J. Mol. Sci. 17 (2016).

[6] L. Gopalakrishnan, K. Doriya, D.S. Kumar, Moringa oleifera: A review on nutritive importance and its medicinal application, Food Science and Human Wellness 5 (2016) 49–56.

[7] A. Jain, R. Subramanian, B. Manohar, C. Radha, Preparation, characterization and functional properties of Moringa oleifera seed protein isolate, J Food Sci Technol 56 (2019) 2093–2104.

[8] M.A. Mune Mune, C.B. Bakwo Bassogog, E.C. Nyobe, S.R. René Minka, F. Yildiz, Physicochemical and functional properties of Moringa oleifera seed and leaf flour, Cogent Food & Agriculture, 2 (2016).

[9] T.G. Kebede, S. Dube, M.M. Nindi, Characterisation of water-soluble protein powder and optimisation of process parameters for the removal of sulphonamides from wastewater, Environ Sci Pollut Res Int, 26 (2019) 21450-21462.

[10] M.T. Mohd Khairi, S. Ibrahim, M.A. Md Yunus, M. Faramarzi, Contact and non-contact ultrasonic measurement in the food industry: a review, Meas. Sci. Technol. 27 (2016).

[11] X. Ren, C. Li, F. Yang, Y. Huang, C. Huang, K. Zhang, L. Yan, Comparison of hydrodynamic and ultrasonic cavitation effects on soy protein isolate functionality, J. Food Eng. 265 (2020) 109697, https://doi.org/10.1016/j.jfoodeng.2019.109697.

[12] Z.Y. Dong, M.Y. Li, G. Tian, T.H. Zhang, H. Ren, S.Y. Quek, Effects of ultrasonic pretreatment on the structure and functionality of chicken bone protein prepared by enzymatic method, Food Chem 299 (2019), 125103.

[13] C. Zhou, H. Ma, X. Yu, B. Liu, G. Yagoub Ael, Z. Pan, Pretreatment of defatted wheat germ proteins (by-products of flour mill industry) using ultrasonic horn and bath reactors: effect on structure and preparation of ACE-inhibitory peptides, Ultrason Sonochem 20 (2013) 1390–1400.

[14] N.A. Mir, C.S. Riar, S. Singh, Physicochemical, molecular and thermal properties of high-intensity ultrasound (HIUS) treated protein isolates from album (Chenopodium album) seed, Food Hydrocolloids 96 (2019) 433–441.

[15] F. Xue, C. Zhu, F. Liu, S. Wang, H. Liu, C. Li, Effects of high-intensity ultrasound treatment on functional properties of plum (Pruni domesticae semen) seed protein isolate, J Sci Food Agric 98 (2018) 5690–5699.

[16] S. Li, H. Ma, Y. Guo, A.O. Oladejo, X. Yang, Q. Liang, Y. Duan, A new kinetic model of ultrasound-assisted pretreatment on rice protein, Ultrason. Sonochem. 40 (2018) 644–650.

[17] A.B. Khatkar, A. Kaur, S.K. Khatkar, N. Mehta, Optimization of processing time, amplitude and concentration for ultrasound-assisted modification of whey protein using response surface methodology, Journal of Food Science and Technology-Mysore 55 (2018) 2298–2309.

[18] S. Jiang, J. Ding, J. Andrade, T.M. Rababah, A. Almajwal, M.M. Abulmeaty, H. Feng, Modifying the physicochemical properties of pea protein by pH-shifting and ultrasound combined treatments, Ultrason Sonochem 38 (2017) 835–842.

[19] J. O'Sullivan, M. Park, J. Beevers, The effect of ultrasound upon the physicochemical and emulsifying properties of wheat and soy protein isolates, J. Cereal Sci. 69 (2016) 77–84.

[20] C. Ozuna, I. Paniagua-Martínez, E. Castaño-Tostado, L. Ozimek, S.L. Amaya-Llano, Innovative applications of high-intensity ultrasound in the development of functional food ingredients: Production of protein hydrolysates and bioactive peptides, Food Res. Int. 77 (2015) 685–696.

[21] J. Chandrapala, B. Zisu, M. Palmer, S. Kentish, M. Ashokkumar, Effects of ultrasound on the thermal and structural characteristics of proteins in reconstituted whey protein concentrate, Ultrason Sonochem 18 (2011) 951–957.

[22] I.H. Han, B.G. Swanson, B.-K. Baik, Protein digestibility of selected legumes treated with ultrasound and high hydrostatic pressure during soaking, Cereal Chem. 84 (2007) 518–521.

[23] T.-K. Kim, H.I. Yong, C.H. Jeong, S.G. Han, Y.-B. Kim, H.-D. Paik, Y.-S. Choi, Technical Functional Properties of Water- and Salt-soluble Proteins Extracted from Edible Insects, Food Sci Anim Resour 39 (4) (2019) 643–654.

[24] B. Ling, S. Ouyang, S. Wang, Effect of radio frequency treatment on functional, structural and thermal behaviors of protein isolates in rice bran, Food Chem. 289 (2019) 537–544.

[25] L.B. Pham, B. Wang, B. Zisu, B. Adhikari, Covalent modification of flaxseed protein isolate by phenolic compounds and the structure and functional properties of the adducts, Food Chem. 293 (2019) 463–471.

[26] M.M. Bradford, A Rapid and Sensitive Method for the Quantitation of Microgram Quantities of Protein Utilizing the Principle of Protein-Dye Binding, Anal Biochem 72 (1976) 248–254.

[27] E. Arte, X. Huang, E. Nordlund, K. Katina, Biochemical characterization and technofunctional properties of bioprocessed wheat bran protein isolates, Food Chem. 289 (2019) 103–111.

[28] D. Li, Y. Zhao, X. Wang, H. Tang, N. Wu, F. Wu, D. Yu, W. Elfalleh, Effects of (+)-catechin on a rice bran protein oil-in-water emulsion: Droplet size, zeta-potential, emulsifying properties, and rheological behavior, Food Hydrocolloid 98 (2020), 105306.

[29] P.B. Stathopulos, G.A. Scholz, Y.M. Hwang, J.A. Rumfeldt, J.R. Lepock, E. M. Meiering, Sonication of proteins causes formation of aggregates that resemble amyloid, Protein Sci 13 (2004) 3017–3027.

[30] X. Tang, B. Kong, Q. Liu, J. Han, Studies on Properties of Soybean Protein Isolate Mixed Gelation with Starches by High-pressure Homogenization, Journal of Chinese Institute Of Food Science and Technology 16 (2016) 68–76.

[31] A.R. Jambrak, T.J. Mason, V. Lelas, G. Krešić, Ultrasonic effect on physicochemical and functional properties of α-lactalbumin, LWT - Food Science and Technology 43 (2010) 254–262.

[32] M.A. Malik, H.K. Sharma, C.S. Saini, High intensity ultrasound treatment of protein isolate extracted from dephenolized sunflower meal: Effect on physicochemical and functional properties, Ultrason. Sonochem. 39 (2017) 511–519.

[33] O.A. Higuera-Barraza, W. Torres-Arreola, J.M. Ezquerra-Brauer, F.J. Cinco-Moroyoqui, J.C. Rodríguez Figueroa, E. Marquez-Ríos, Effect of pulsed ultrasound on the physicochemical characteristics and emulsifying properties of squid (Dosidicus gigas) mantle proteins, Ultrason. Sonochem. 38 (2017) 829–834.

[34] L. Chen, J. Chen, K. Wu, L. Yu, Improved Low pH Emulsification Properties of Glycated Peanut Protein Isolate by Ultrasound Maillard Reaction, J Agric Food Chem 64 (2016) 5531–5538.

[35] B. Nazari, M.A. Mohammadifar, S. Shojaee-Aliabadi, E. Feizollahi, L. Mirmoghtadaie, Effect of ultrasound treatments on functional properties and structure of millet protein concentrate, Ultrason. Sonochem. 41 (2018) 382–388.
[36] H. Hu, I.W.Y. Cheung, S. Pan, E.C.Y. Li-Chan, Effect of high intensity ultrasound on physicochemical and functional properties of aggregated soybean β-conglycinin and glycinin, Food Hydrocolloids 45 (2015) 102–110.
[37] F. Yang, X. Liu, X.e. Ren, Y. Huang, C. Huang, K. Zhang, Swirling cavitation improves the emulsifying properties of commercial soy protein isolate, Ultrasonics Sonochemistry, 42 (2018) 471-481.